bioRxiv preprint doi: https://doi.org/10.1101/2020.07.21.214577; this version posted October 21, 2020. The copyright holder for this preprint (which was not certified by peer review) is the author/funder, who has granted bioRxiv a license to display the preprint in perpetuity. It is made available under aCC-BY-NC-ND 4.0 International license.

FDA approved calcium channel blockers inhibit SARS-CoV-2 infectivity in epithelial lung cells

Marco R. Straus[1], Miya Bidon[2], Tiffany Tang[2], Gary R. Whittaker[1*] and Susan Daniel[2*]

[1]Department of Microbiology and Immunology, Cornell University, Ithaca, NY, 14853, USA

[2]Robert Frederick Smith School of Chemical and Biomolecular Engineering, Cornell University, Ithaca, NY, 14853, USA

*Corresponding authors:

Gary Whittaker: grw7@cornell.edu

Susan Daniel: sd386@cornell.edu

Abstract

COVID-19 has infected more than 41 million people worldwide with over 1.1 million deaths and is caused by the severe acute respiratory syndrome coronavirus (CoV) 2 (SARS-CoV-2)(1). Currently there are no protective vaccinations available and the only antiviral therapy in active use in patients is remdesivir, which provides only limited benefit(2, 3). Hence, an urgent need for antiviral therapies against SARS-CoV-2 exists. SARS-CoV requires Ca^{2+} ions for host cell entry and based on the similarity between SARS-CoV and SARS-CoV-2 it is highly likely that the same requirements exist for both viruses(4, 5). Here, we tested whether FDA-approved calcium channel blocker (CCB) drugs can inhibit SARS-CoV-2 infection in cell culture. All the CCBs showed varying degrees of inhibition, with amlodipine and nifedipine strongly limiting SARS-CoV-2 entry and infection in epithelial lung cells at concentrations where cell toxicity was minimal. Further studies with pseudo-typed particles carrying the SARS CoV 2 Spike protein suggest that viral inhibition occurs at the level of viral host cell entry. Overall, our data

bioRxiv preprint doi: https://doi.org/10.1101/2020.07.21.214577; this version posted October 21, 2020. The copyright holder for this preprint (which was not certified by peer review) is the author/funder, who has granted bioRxiv a license to display the preprint in perpetuity. It is made available under aCC-BY-NC-ND 4.0 International license.

suggest that CCBs have a high potential to treat SARS-CoV-2 infections and their current FDA approval would allow for a fast repurposing of these drugs.

Significance

Covid-19 infections are still increasing around the globe and a number of countries are currently facing a second wave of infection resulting in re-instated lockdowns and dramatic consequences for the public health systems. Vaccine developments are in progress but as of now there are no efficacious drugs on the market to fight the pandemic. Here, we present the first case of a FDA-approved class of drugs that inhibit SARS CoV 2 growth *in vitro*. Their FDA approval may reduce the time for repurposing, allowing bypass of time- and cost-intensive animal models and to test them directly in clinical trials for human application for treatment of Covid-19.

Introduction

Coronaviruses (CoVs) are major zoonotic pathogens that cause respiratory and/or enteric tract infections in a variety of species, including humans. Most CoVs that are pathogenic to humans cause only mild cold-like disease symptoms(6). However, currently the worldwide COVID-19 pandemic is caused by the severe acute respiratory syndrome (SARS) CoV 2 and poses a dramatic risk to public health worldwide(7). The virus was first identified in December 2019 in Wuhan, China and since has spread all over the globe(8). To date, there are no vaccines or highly efficacious drugs available against SARS-CoV-2.

Early during the pandemic chloroquine and hydroxychloroquine were promoted as efficacious treatments against Covid-19. But a recent report dismissed both drugs showing that they suppress viral

bioRxiv preprint doi: https://doi.org/10.1101/2020.07.21.214577; this version posted October 21, 2020. The copyright holder for this preprint (which was not certified by peer review) is the author/funder, who has granted bioRxiv a license to display the preprint in perpetuity. It is made available under aCC-BY-NC-ND 4.0 International license.

growth in the epithelial kidney cell line Vero E6 but not in the relevant epithelial lung Calu-3 cells (9). Remdesivir, initially developed for Ebola treatment, is currently the only antiviral therapy used to effectively treat COVID-19 patients and was shown to improve symptoms in 68% of treated patients in clinical trials(2, 3). However, with only one efficacious antiviral therapy on the market, there remains a need to identify and to provide additional drugs that can treat COVID-19 patients. Given the current pandemic and the need for expediency, these drugs should ideally be FDA approved so they can be rapidly repurposed for COVID-19 treatment.

A promising target for a potential drug is a crucial step in the viral life cycle, such as the entry of the virus into the host cells(5). Previous studies have revealed that SARS-CoV and MERS-CoV utilize calcium ions (Ca^{2+}) for viral entry that are coordinated by amino acid residues within the fusion peptide of their Spike (S) proteins(4, 10). Depleting intracellular and/or extracellular Ca^{2+} resulted in full suppression of viral entry for SARS-CoV and partial reduction of viral fusion of MERS-CoV. Sequence comparisons show that the fusion domains of SARS-CoV and SARS-CoV-2 are virtually identical, strongly suggesting that the same Ca^{2+}-dependency for viral entry exists for SARS-CoV-2(5).

The crucial role of Ca^{2+} in the viral entry of CoVs prompted us to explore whether FDA approved Ca^{2+} channel blocker (CCB) drugs have the potential to inhibit viral growth of SARS-CoV-2. We chose five drugs from different classes that all inhibit high voltage-activated Ca^{2+} channels of the L-type. We selected the dihydropyridines: amlodipine, nifedipine and felodipine; the phenylalkylamine: verapamil; and the benzothiazepine: diltiazem. These five drugs are primarily used to treat cardio-vascular diseases. In addition, we also tested the FDA-approved Ca^{2+} chelator drug: diethylenetriaminepentaacetic acid (DTPA), which is used to treat radioactive contamination of internal organs.

Results and Discussion

bioRxiv preprint doi: https://doi.org/10.1101/2020.07.21.214577; this version posted October 21, 2020. The copyright holder for this preprint (which was not certified by peer review) is the author/funder, who has granted bioRxiv a license to display the preprint in perpetuity. It is made available under aCC-BY-NC-ND 4.0 International license.

We infected Vero E6 cells at a MOI of 0.1 and added four different concentrations of each compound immediately post infection (10 µM, 50 µM, 100 µM and 500 µM). Viral titers were analyzed 24 hours post infection. For amlodipine, we observed a 5-log reduction of viral growth at 50 µM and we were not able to detect any viral titer at a concentration of 100 µM (Figure 1A). However, amlodipine also exhibited a 25% reduction of cell viability at a concentration of 50 µM, which increased to 90% at 100 µM and 500 µM (Figure 1A). Nifedipine reduced viral titers by 5 logs at 500 µM and expressed about 15% cytotoxicity (Figure 1B). Felodipine completely suppressed growth of SARS-CoV-2 at a concentration of 50 µM with no statistically significant cytotoxicity (Figure 1C). 100 µM verapamil reduced the viral titers by 50% compared to the untreated control without a cytotoxic effect (Figure 1D). Diltiazem reduced viral growth at 500 µM but also compromised cell viability at this concentration and DTPA showed no effect Figure 1E and 1F).

Vero E6 cells are a good model system for SARS-CoV-2 infections, but the cell line is derived from epithelial kidney cells and may not represent the virus-drug-cell interactions in the lung. Therefore, we tested the CCBs and DTPA in the epithelial lung cell line Calu-3 (Figure 2). The results for amlodipine were comparable to what we found in Vero E6 cells (Figure 1A and 2A). Nifedipine and felodipine, however, significantly inhibited viral growth at lower concentrations compared to Vero E6 cells (Figure 2B and 2C). Nifedipine reduced the viral titers by 1.5 logs at a concentration of 100 µM and no virus was detectable at 500 µM while cytotoxicity was moderate (Figure 2B). Felodipine diminished SARS-CoV-2 growth by half at 10 µM and at 50 µM no virus was detected with no cytotoxic effect on the cells (Figure 2C). In contrast, verapamil had a weakened inhibitory effect at 100 µM compared to Vero E6 cells (Figure 2D). As in Vero E6 cells, 100 µM verapamil fully suppressed viral growth but also compromised cell viability by about 90%. We found very modest infection inhibition for diltiazem and DTPA at non-cytotoxic concentrations of 500 µM and 100 µM, respectively (Figure 2E and 2F).

bioRxiv preprint doi: https://doi.org/10.1101/2020.07.21.214577; this version posted October 21, 2020. The copyright holder for this preprint (which was not certified by peer review) is the author/funder, who has granted bioRxiv a license to display the preprint in perpetuity. It is made available under aCC-BY-NC-ND 4.0 International license.

With Amlodipine, Felodipine and Nifedipine being the most promising candidates that suppressed SARS CoV 2 growth in epithelial lung cells we aimed to determine their selectivity index (SI). The SI provides a measure how safe a given drug would be for the treatment of SARS CoV 2 infections *in vivo*. To calculate the SI we determined for each of the three drugs at which concentration they inhibit 50% of the viral growth (EC_{50}) and the concentration at which each drug exerts 50% cytotoxicity (CC_{50}). Dividing CC_{50}/EC_{50} results in the SI and the higher the SI the more selective the drug is against the pathogen. However, it has to be emphasized that the SI determined here serves as an indicator and provides important information to consider for human application but the final efficacy in humans may differ and potential side effects of the drugs cannot be taken into account. Calu-3 cells as the more relevant cell line compared to Vero cells were infected with SARS CoV 2 and different concentrations of the respective drugs were applied (SI Figure 1). The obtained EC_{50} values were 10.36 µM for Amlodipine, 0.01255 µM for Felodipine and 20.47 µM for Nifedipine (SI Figure 1A - C, Table 1). We determined the CC_{50}s in a similar fashion using a cytotoxicity assay as described above resulting in CC_{50} values of 27.85 µM for Amlodipine and 122.8 µM for Felodipine (SI Figure 1A and B). For Nifedipine the highest tested concentration of 2 mM did not significantly impair cell viability (SI Figure 1C, Table 1). The obtained SI values were 2.69 for Amlodipine and 9784.86 for Felodipine (Table 1). Because Nifedipine did not show a significant cytotoxic effect at approx. 7x the concentration of the most efficacious antiviral concentration of 300 µM a SI value could not be determined. Hence, all three drugs seem to be very selective against SARS CoV 2 with Felodipine and Nifedipine being the most promising candidates because of their high SI score and very low cytotoxicity, respectively.

It is important to emphasize that felodipine and nifedipine work with higher efficiency in Calu-3 cells compared to Vero E6 cells (Figure 1 and 2). In this context, it is noteworthy that CCBs are believed to affect airway smooth muscle cells, which rely on L-type calcium channels for their contraction(11–13). Recently, the same CCBs tested here were shown to have a beneficial effect on the lung function of

bioRxiv preprint doi: https://doi.org/10.1101/2020.07.21.214577; this version posted October 21, 2020. The copyright holder for this preprint (which was not certified by peer review) is the author/funder, who has granted bioRxiv a license to display the preprint in perpetuity. It is made available under aCC-BY-NC-ND 4.0 International license.

asthma patients, providing evidence that CCBs act in the lungs(14). More evidence that interference with the cellular Ca^{2+} balance suppresses viral growth comes from nebulizers used for asthma medications. Nebulizers are supplemented with EDTA as a preservative, which may help to deplete extracellular Ca^{2+}(15) and provide a clue as to why asthma is not on the top ten list of chronic health problems of people who died of COVID-19.

The observed inhibition differences in these two cell lines suggest that inhibition may occur at the level of host cell entry. In Vero cells, CoVs preferentially enter the host cells via the endocytic pathway (5, 16). Calu-3 cells, on the contrary, are predominantly infected via plasma membrane fusion(5, 17). To further investigate whether CCB-mediated inhibition of SARS-CoV-2 infectivity affects viral host cell entry, we utilized murine leukemia virus (MLV)-based pseudo particles (PP) that were decorated with the SARS-CoV-2 S protein(18). These virion surrogates allow for only one infection cycle without intracellular replication and thus, inhibition of PP infection would suggest that the CCBs affect host cell entry.

We pretreated all cells with the CCBs and DTPA for one hour before adding PPs carrying the SARS-CoV-2 S protein (Figure 3). Amlodipine suppressed PP infection at 50 µM in both, Vero E6 and Calu-3 cells (Figure 3). Nifedipine inhibited PP infection in Vero E6 and Calu-3 cells with 500 µM having the strongest effect. Felodipine inhibited PP entry in both cell lines at 50 µM. Consistent with what we found in the live virus infection study above, verapamil suppressed PP entry at 50 µM in Calu-3 and at 100 µM in Vero E6 cells. In contrast to our observations with SARS-CoV-2 live virus infections, diltiazem and DTPA also inhibited PP infections (Figure 1, 2 and 3). Diltiazem inhibited PP infection in Calu-3 starting at 50 µM, and in Vero E6, at 500 µM. DTPA had a much stronger effect, suggesting that it might be able to chelate Ca^{2+} ions in the extracellular space, and thus, prevent fusion of S with the membrane as previously described for SARS-CoV PPs in the presence of EGTA(4). The applied DTPA concentrations, however, seem sufficient to prevent a single host cell entry, but incapable of inhibiting SARS-CoV-2 spread over several rounds of viral replication under the conditions used here.

bioRxiv preprint doi: https://doi.org/10.1101/2020.07.21.214577; this version posted October 21, 2020. The copyright holder for this preprint (which was not certified by peer review) is the author/funder, who has granted bioRxiv a license to display the preprint in perpetuity. It is made available under aCC-BY-NC-ND 4.0 International license.

There is evidence from previous reports that CCBs inhibit viral infections at the cell entry level. Influenza A infections, for example, trigger an influx of Ca^{2+} which assists the endocytic uptake of the virus, while treatment with verapamil or diltiazem inhibits viral infection(19–21). New World hemorrhagic fever arenaviruses, such as the Junin virus, are reportedly sensitive to CCBs and treatment with CCBs blocks the entry of the virus into the host cell(22). However, the exact mechanism of how CCBs suppress SARS-CoV-2 infection needs to be addressed in a follow up study. CCBs were also shown to interfere with viral replication of several other viruses (*e.g.,* Japanese Encephalitis virus, Zika virus, Dengue virus)(23). Hence, while our results point to an interference of SARS-CoV-2 at host cell entry, it is conceivable that CCB-mediated inhibition of viral spread occurs at other stages as well, including viral release. It will require further studies to determine whether CCBs interfere directly with virus-cell fusion, how these drugs may affect the different fusion pathways and to explore whether CCBs may inhibit other cell functions that subsequently lead to inhibition of host cell entry. Regardless of the exact mechanism, these examples demonstrate that CCBs exhibit an antiviral efficacy against a broad range of viral pathogens relevant for public health. They also show the broad requirement of Ca^{2+} ions for viral propagation, supported by other studies that report a Ca^{2+} requirement for major human pathogens like Ebola virus and Rubella virus(24, 25). Therefore, CCBs may represent a novel class of antiviral therapeutics against a broad range of major viral diseases that warrant further clinical studies, but especially to address the current crisis of Covid-19.

In summary, the results described above are promising and particularly Felodipine and Nifedipine may represent a viable treatment option against Covid-19. However, it is unclear how the efficacious doses found here and the SI score would translate into clinical use in human patients to treat Covid-19 infections. As a next step, a meta-analysis of patient data taking CBBs medication and the relation to the severity of Covid-19 (e.g. hospitalizations, intubations etc.) in these patients may provide further insights about the efficacy of CBBs to inhibit SARS CoV 2 in humans.

bioRxiv preprint doi: https://doi.org/10.1101/2020.07.21.214577; this version posted October 21, 2020. The copyright holder for this preprint (which was not certified by peer review) is the author/funder, who has granted bioRxiv a license to display the preprint in perpetuity. It is made available under aCC-BY-NC-ND 4.0 International license.

Figure legends

Figure 1: Inhibitory effect of five CCBs and the Ca^{2+} chelator DTPA on SARS-CoV-2 infection and correlation to cell viability in Vero E6 cells. (Infectivity A-E) Vero E6 epithelial kidney cells were infected with SARS-CoV-2 isolate USA-WA1/2020 at a MOI of 0.1 for 24 hours. The CCBs amlodipine, nifedipine, felodipine, verapamil and diltiazem and the chelator DTPA were added to the cells at the indicated concentrations immediately after the virus. 0 µM sample contained only DMSO which was used as solvent for the drugs. TCID50s were performed with growth supernatants and calculated according to the Reed-Muench method(26). No bar means no virus was detected at the respective concentration. Error bars represent standard deviations (n = 3). Asterisks indicate statistical significance compared to the untreated control. Statistical analysis was performed using an unpaired Student's t-test. * = P > 0.05, ** = P > 0.01, *** = P > 0.001. **(Cell viability A-F)** Vero E6 epithelial kidney cells were treated with the indicated concentrations of amlodipine, nifedipine, felodipine, verapamil, diltiazem and DTPA for 24 hours. After 24 hours cell viability was measured using 3-(4,5-dimethylthiazol-2-yl)-2,5-diphenyltetrazolium bromide (MTT). Cell viability was determined by normalizing absorbance from the sample well by the average absorbance of untreated wells. As for the infections, 0 µM sample contained only DMSO which was used as solvent for the drugs. Error bars represent standard deviations (n = 3). Asterisks indicate statistical significance compared to the untreated control. Statistical analysis was performed using an unpaired Student's t-test. * = P > 0.05, ** = P > 0.01, *** = P > 0.001.

Figure 2: Inhibitory effect of five CCBs and the Ca^{2+} chelator DTPA on SARS-CoV-2 infection and correlation to cell viability in Calu-3 cells. Conditions for **(Infectivity A-F)** and **(Cell viability A-F)** in Calu-3 epithelial lung cells as described in figure legend Figure 1. Error bars represent standard deviations (n

bioRxiv preprint doi: https://doi.org/10.1101/2020.07.21.214577; this version posted October 21, 2020. The copyright holder for this preprint (which was not certified by peer review) is the author/funder, who has granted bioRxiv a license to display the preprint in perpetuity. It is made available under aCC-BY-NC-ND 4.0 International license.

= 3). Asterisks indicate statistical significance compared to the untreated control. Statistical analysis was performed using an unpaired Student's t-test. * = P > 0.05, ** = P > 0.01, *** = P > 0.001.

Figure 3: Pseudo particle assays of SARS-CoV-2 S in Vero E6 and Calu-3 cells. (A) Vero E6 epithelial kidney cells and (B) Calu-3 epithelial lung cells were pre-treated with CCBs and DTPA for one hour prior to infection with PPs carrying SARS-CoV-2 S. After 24 hours growth medium was changed and replenished with the drugs. 72 hours after infection the luciferase activity was assessed. Infectivity was normalized to the untreated sample. Error bars represent standard deviations (n = 3). Asterisks indicate statistical significance compared to the untreated control. Statistical analysis was performed using an unpaired Student's t-test. * = P > 0.05, ** = P > 0.01, *** = P > 0.001.

Table 1: EC_{50}, CC_{50} and Selectivity Index (SI) of Amlodipine, Felodipine and Nifedipine. EC_{50} and CC_{50} were determined in Calu-3 cells. SI = CC_{50}/EC_{50}.

SI Figure 1: Determination of EC_{50} and CC_{50} of Amlodipine, Felodipine and Nifedipine in Calu-3 cells. Calu-3 epithelial lung cells cells were infected with SARS-CoV-2 isolate USA-WA1/2020 at a MOI of 0.1 for 24 hours. The CCBs amlodipine (A) and felodipine (B) were added to the cells at the 0, 10, 20, 30, 40 and 50 µM immediately after the virus. Nifedipine (C) was added at concentrations of 50, 75, 100, 200, 300, 400 and 500 µM. TCID50s were performed with growth supernatants and calculated according to the Reed-Muench method(26). Cell viability was measured using 3-(4,5-dimethylthiazol-2-yl)-2,5-diphenyltetrazolium bromide (MTT). Cell viability was determined by normalizing absorbance from the sample well by the average absorbance of untreated wells. Drug concentrations were converted into log10 numbers and plotted on the x-axis. EC_{50} and CC_{50} values were calculated using Graphpad Prism 8 software. Error bars represent standard deviations (n = 3).

Methods

Cells and reagents

bioRxiv preprint doi: https://doi.org/10.1101/2020.07.21.214577; this version posted October 21, 2020. The copyright holder for this preprint (which was not certified by peer review) is the author/funder, who has granted bioRxiv a license to display the preprint in perpetuity. It is made available under aCC-BY-NC-ND 4.0 International license.

Vero E6 and Calu-3 cells were obtained from the American Type Culture Collection (ATCC). Cells were maintained in Dulbecco's modified Eagle medium (DMEM) (Cellgro) supplemented with 25 mM HEPES (Cellgro) and 10% HyClone FetalClone II (GE) at 37° C and 5% CO_2. For virus infections, cells were grown in Eagle's Minimum Essential Medium (EMEM) (Cellgro) supplemented with 4% heat inactivated fetal bovine serum (FBS) (Gibco) at 37° C and 5% CO_2.

The SARS-CoV-2 isolate USA-WA1/2020 was obtained from the Biological and Emerging Infections Resources Program (BEI Resources). Amlodipine, nifedipine, felodipine, verapamil, diltiazem and DTPA were purchased from Sigma Aldrich. 3-(4,5-dimethylthiazol-2-yl)-2,5-diphenyltetrazolium bromide (MMT) was obtained from Thermo Fisher. Crystal violet was purchased from VWR. pCDNA3.1/SARS-CoV-2 S Wuhan Hu-1 was generously provided by Dr. David Veesler.

SARS-CoV-2 infections and TCID50 assays

Vero E6 and Calu-3 cells were grown to confluency under biosafety level-2 (BSL-2) conditions. Cells were then transferred to the BSL-3 lab, washed with DBPS and a volume of 200 µL infection media with SARS-CoV-2 at a MOI of 0.1 was added to the cells. Cells were then incubated at 37° C and 5% CO_2 for 1 hour on a rocker. Cells were then supplemented with 800 µL infection media and appropriate concentrations of each drug were added. Amlodipine, nifedipine, felodipine and verapamil were dissolved in DMSO. Therefore, DMSO was used as a control at the same volume that was applied for the highest drug concentration. After 24 hours, the supernatants were harvested and stored at -80° C.

For the TCID50, Vero E6 cells were grown to confluency in 96 well plates and serial dilution of the samples were prepared. Undiluted and diluted samples were then added to the Vero E6 cells and grown for 72 hours at 37° C and 5% CO_2. After 72 hours supernatants were aspirated, and cells were fixed with 4% paraformaldehyde. Cells were then stained with 0.5% crystal violet and subsequently washed with

bioRxiv preprint doi: https://doi.org/10.1101/2020.07.21.214577; this version posted October 21, 2020. The copyright holder for this preprint (which was not certified by peer review) is the author/funder, who has granted bioRxiv a license to display the preprint in perpetuity. It is made available under aCC-BY-NC-ND 4.0 International license.

dH_2O. Wells were scored and analyzed for living or dead cells according to the Reed-Muench method(26).

Cytotoxicity assay

The cytotoxicity of the calcium ion blocking drugs (amlodipine, nifedipine, felodipine, diltiazem) and calcium chelator (DTPA) on VeroE6 and Calu-3 cells were determined by an MTT Assay. A total of 5×10^5 VeroE6 cells/well, and 6.7×10^5 Calu-3 cells/well were incubated in the presence of the six calcium blocking drugs and calcium chelator at the concentrations of 10, 50, 100, and 500 µM for 24 hour at 37°C C and 5% CO_2 in a CO_2 incubator. After 24 hours incubation, cells were treated with MTT solution (5 mg/mL) and incubated for 4 hours at 37°C and 5% CO_2 with rocking to allow purple formazan crystals to form. 50 µL DMSO was added into each well to dissolve the crystals. The absorbance was measured at 540 nm in a microplate reader (Bio-Tek Instrument Co., WA, USA).

Pseudo particle production and infections

Pseudo particles production and infections were performed as previously described with minor modification(10). For PP production, HEK 293T cells were transfected with pCDNA3.1/SARS-CoV-2 S Wuhan Hu-1 to generate SARS-CoV-2 S carrying PPs. Supernatants were harvested 72 hours post transfection and stored at -80°C. For infections, cells were seeded in 96-well plates and DMEM containing the different CCBs and DTPA was added and incubated for 1 hour. After one hour 50 µL PPs were added. After 24 hours, cells were replenished with DMEM containing the individual drugs at the appropriate concentration and incubated for another 48 hours. After lysis, luciferase activity was measured using a GloMax Navigator Microplate Luminometer (Promega). Data was analyzed using Microsoft Excel and GraphPad Prism 8.

bioRxiv preprint doi: https://doi.org/10.1101/2020.07.21.214577; this version posted October 21, 2020. The copyright holder for this preprint (which was not certified by peer review) is the author/funder, who has granted bioRxiv a license to display the preprint in perpetuity. It is made available under aCC-BY-NC-ND 4.0 International license.

References

1. E. Dong, H. Du, L. Gardner, An interactive web-based dashboard to track COVID-19 in real time. *Lancet Infect. Dis.* **20**, 533–534 (2020).

2. J. Grein, *et al.*, Compassionate Use of Remdesivir for Patients with Severe Covid-19. *N. Engl. J. Med.* **382**, 2327–2336 (2020).

3. D. R. Boulware, *et al.*, A Randomized Trial of Hydroxychloroquine as Postexposure Prophylaxis for Covid-19. *N. Engl. J. Med.* **383**, 517–525 (2020).

4. A. L. Lai, J. K. Millet, S. Daniel, J. H. Freed, G. R. Whittaker, The SARS-CoV Fusion Peptide Forms an Extended Bipartite Fusion Platform that Perturbs Membrane Order in a Calcium-Dependent Manner. *J. Mol. Biol.* **429**, 3875–3892 (2017).

5. T. Tang, M. Bidon, J. A. Jaimes, G. R. Whittaker, S. Daniel, Coronavirus membrane fusion mechanism offers a potential target for antiviral development. *Antiviral Res.* **178** (2020).

6. S. Su, *et al.*, Epidemiology, Genetic Recombination, and Pathogenesis of Coronaviruses. *Trends Microbiol.* **24**, 490–502 (2016).

7. World Health Organization, "Coronavirus Disease 2019 (COVID-19) Situation Reports - 72" (2020) (July 14, 2020).

8. F. Wu, *et al.*, A new coronavirus associated with human respiratory disease in China. *Nature* **579**, 265–269 (2020).

9. M. Hoffmann, *et al.*, Chloroquine does not inhibit infection of human lung cells with SARS-CoV-2. *Nature* **585**, 588–590 (2020).

10. M. R. Straus, *et al.*, Ca 2+ Ions Promote Fusion of Middle East Respiratory Syndrome Coronavirus

bioRxiv preprint doi: https://doi.org/10.1101/2020.07.21.214577; this version posted October 21, 2020. The copyright holder for this preprint (which was not certified by peer review) is the author/funder, who has granted bioRxiv a license to display the preprint in perpetuity. It is made available under aCC-BY-NC-ND 4.0 International license.

with Host Cells and Increase Infectivity. *J. Virol.* **94**, 426–446 (2020).

11. C. -G Löfdahl, P. J. Barnes, Calcium, Calcium Channel Blockade and Airways Function. *Acta Pharmacol. Toxicol. (Copenh).* **58**, 91–111 (1986).

12. W. Du, *et al.*, Excitation-contraction coupling in airway smooth muscle. *J. Biol. Chem.* **281**, 30143–30151 (2006).

13. E. Flores-Soto, J. Reyes-García, B. Sommer, L. M. Montaño, Sarcoplasmic reticulum Ca2+ refilling is determined by L-type Ca2+ and store operated Ca2+ channels in guinea pig airway smooth muscle. *Eur. J. Pharmacol.* **721**, 21–28 (2013).

14. K. Y. Chiu, J. G. Li, Y. Lin, Calcium channel blockers for lung function improvement in asthma: A systematic review and meta-analysis. *Ann. Allergy, Asthma Immunol.* **119**, 518-523.e3 (2017).

15. D. P. Cashman, Why the lower reported prevalence of asthma in patients diagnosed with COVID-19 validates repurposing EDTA solutions to prevent and manage treat COVID-19 disease. *Med. Hypotheses* **144**, 110027 (2020).

16. S. Matsuyama, *et al.*, Efficient Activation of the Severe Acute Respiratory Syndrome Coronavirus Spike Protein by the Transmembrane Protease TMPRSS2. *J. Virol.* **84**, 12658–12664 (2010).

17. M. Kawase, K. Shirato, L. van der Hoek, F. Taguchi, S. Matsuyama, Simultaneous Treatment of Human Bronchial Epithelial Cells with Serine and Cysteine Protease Inhibitors Prevents Severe Acute Respiratory Syndrome Coronavirus Entry. *J. Virol.* **86**, 6537–6545 (2012).

18. J. K. Millet, *et al.*, Production of pseudotyped particles to study highly pathogenic coronaviruses in a biosafety level 2 setting. *J. Vis. Exp.* **2019** (2019).

19. Y. Fujioka, *et al.*, A Ca2+-dependent signalling circuit regulates influenza A virus internalization

bioRxiv preprint doi: https://doi.org/10.1101/2020.07.21.214577; this version posted October 21, 2020. The copyright holder for this preprint (which was not certified by peer review) is the author/funder, who has granted bioRxiv a license to display the preprint in perpetuity. It is made available under aCC-BY-NC-ND 4.0 International license.

and infection. *Nat. Commun.* **4**, 1–13 (2013).

20. K. M. Nugent, J. D. Shanley, Verapamil inhibits influenza A virus replication. *Arch. Virol.* **81**, 163–170 (1984).

21. Y. Fujioka, *et al.*, A Sialylated Voltage-Dependent Ca 2+ Channel Binds Hemagglutinin and Mediates Influenza A Virus Entry into Mammalian Cells. *Cell Host Microbe* **23**, 809-818.e5 (2018).

22. M. Lavanya, C. D. Cuevas, M. Thomas, S. Cherry, S. R. Ross, siRNA screen for genes that affect Junín virus entry uncovers voltage-gated calcium channels as a therapeutic target. *Sci. Transl. Med.* **5**, 204ra131-204ra131 (2013).

23. S. Wang, *et al.*, Screening of FDA-Approved Drugs for Inhibitors of Japanese Encephalitis Virus Infection. *J. Virol.* **91** (2017).

24. L. Nathan, *et al.*, Calcium ions directly interact with the Ebola virus fusion peptide to promote structure-function changes that enhance infection. *ACS Infect. Dis.*, acsinfecdis.9b00296 (2019).

25. M. Dubé, F. A. Rey, M. Kielian, Rubella Virus: First Calcium-Requiring Viral Fusion Protein. *PLoS Pathog.* **10** (2014).

26. B. D. Lindenbach, Measuring HCV infectivity produced in cell culture and in vivo. *Methods Mol. Biol.* **510**, 329–336 (2009).

Acknowledgements

This projected was funded by Fast Grant, Mercatus Center. We would like to thank Paul Jeannette for his support for all the BSL-3 work and Dr. Luis Schang, Dr. Nihal Altan-Bonnet, Dr. Fernando Martinez, Dr.

bioRxiv preprint doi: https://doi.org/10.1101/2020.07.21.214577; this version posted October 21, 2020. The copyright holder for this preprint (which was not certified by peer review) is the author/funder, who has granted bioRxiv a license to display the preprint in perpetuity. It is made available under aCC-BY-NC-ND 4.0 International license.

Bruce Kornreich and Dr. Hanno Andreas Ludewig for their critical input. TT is supported by the National Science Foundation Graduate Research Fellowship Program under Grant No. DGE-1650441.

Author contributions

MRS: study design, experimental execution, data analysis, writing and editing of the manuscript. MB: experimental execution and data analysis. TT: experimental execution and data analysis. GRW: study design, writing and editing of the manuscript. SD: study design, writing and editing of the manuscript, funding acquisition.

Figure and Tables

Table 1

	EC_{50} (μM)	CC_{50} (μM)	SI
Amlodipine	10.36	27.85	2.688224
Felodipine	0.01255	122.8	9784.861
Nifedipine	20.47	> NNNN	> NNNN

bioRxiv preprint doi: https://doi.org/10.1101/2020.07.21.214577; this version posted October 21, 2020. The copyright holder for this preprint (which was not certified by peer review) is the author/funder, who has granted bioRxiv a license to display the preprint in perpetuity. It is made available under aCC-BY-NC-ND 4.0 International license.

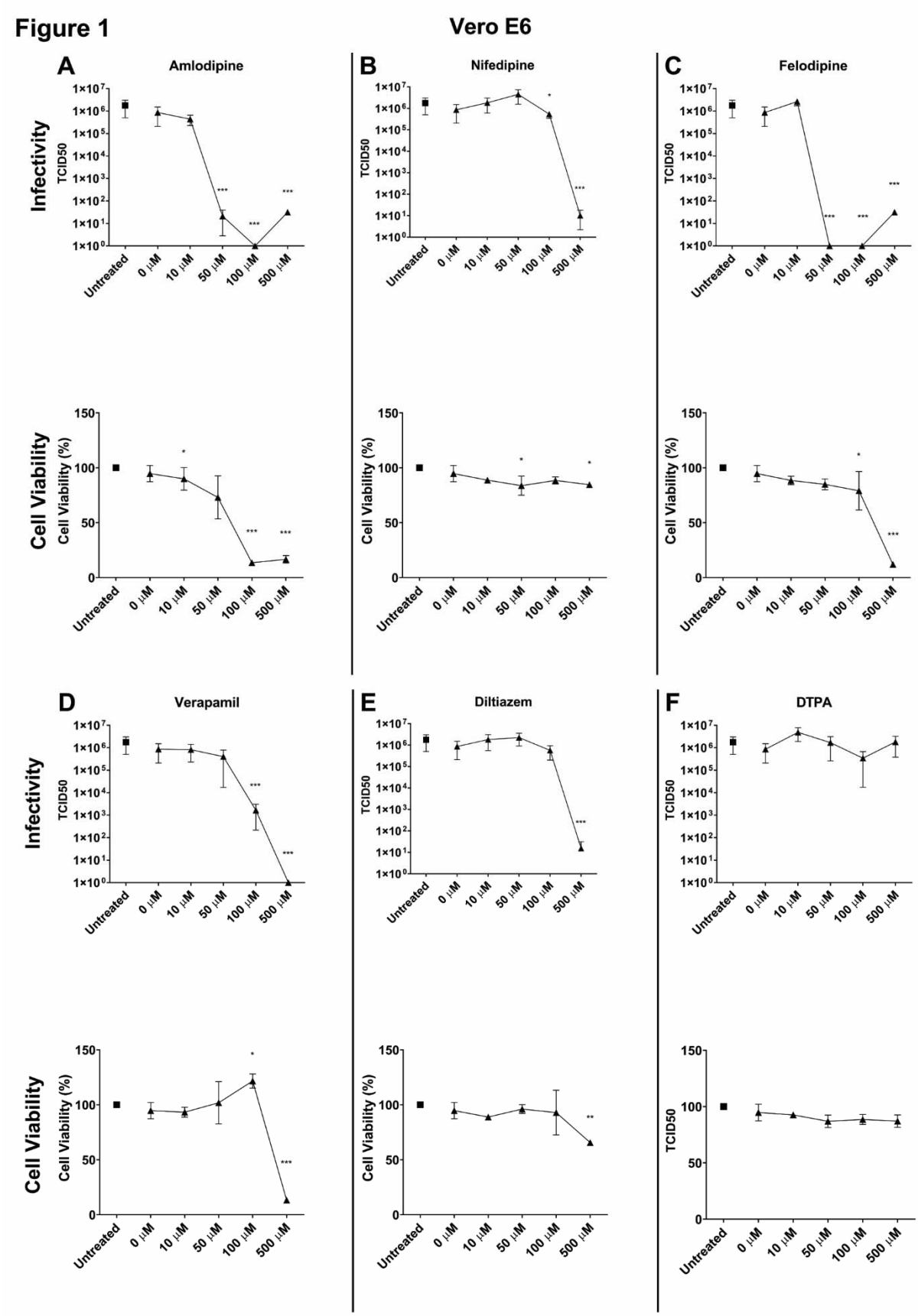

bioRxiv preprint doi: https://doi.org/10.1101/2020.07.21.214577; this version posted October 21, 2020. The copyright holder for this preprint (which was not certified by peer review) is the author/funder, who has granted bioRxiv a license to display the preprint in perpetuity. It is made available under aCC-BY-NC-ND 4.0 International license.

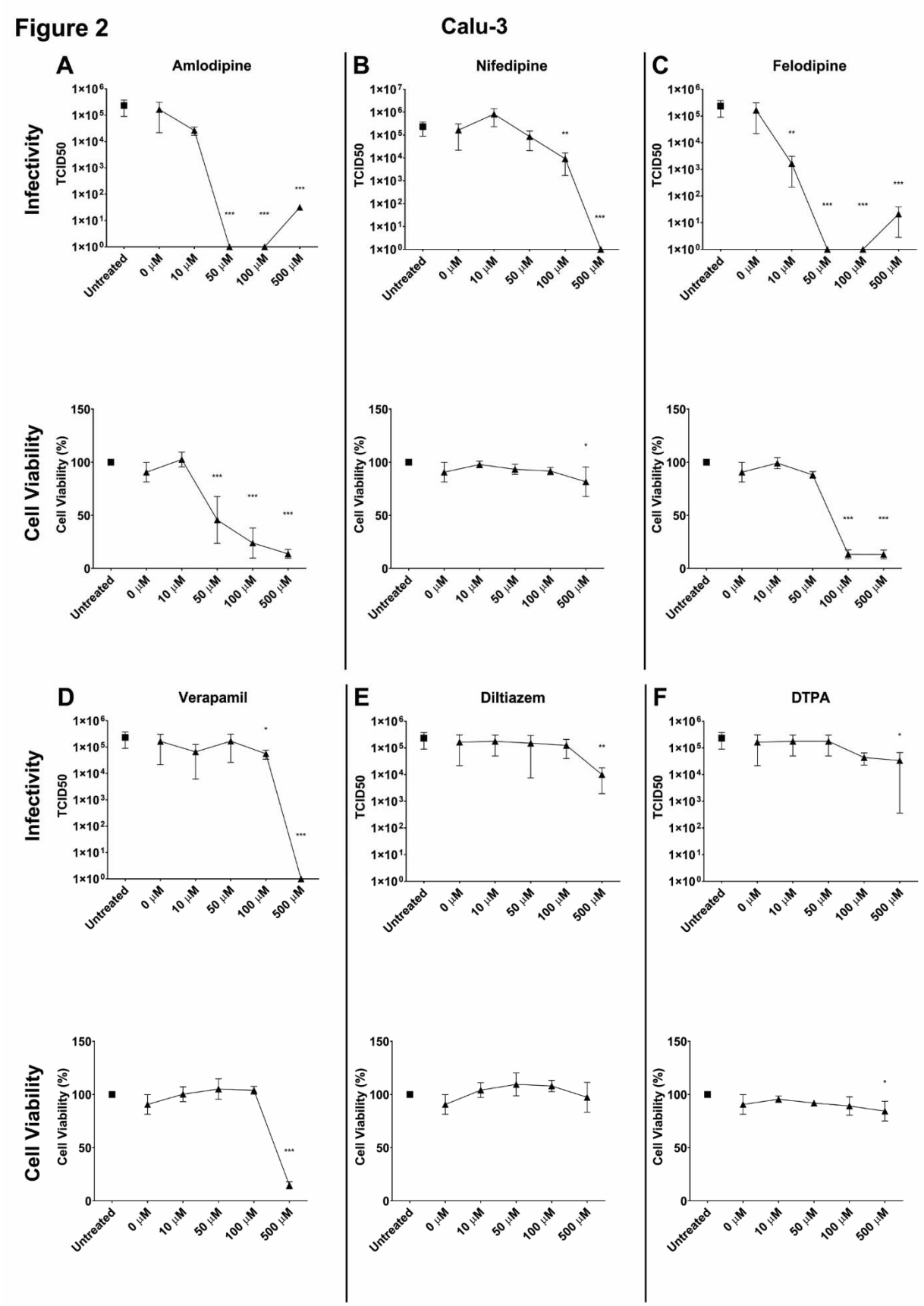

bioRxiv preprint doi: https://doi.org/10.1101/2020.07.21.214577; this version posted October 21, 2020. The copyright holder for this preprint (which was not certified by peer review) is the author/funder, who has granted bioRxiv a license to display the preprint in perpetuity. It is made available under aCC-BY-NC-ND 4.0 International license.

Figure 3A

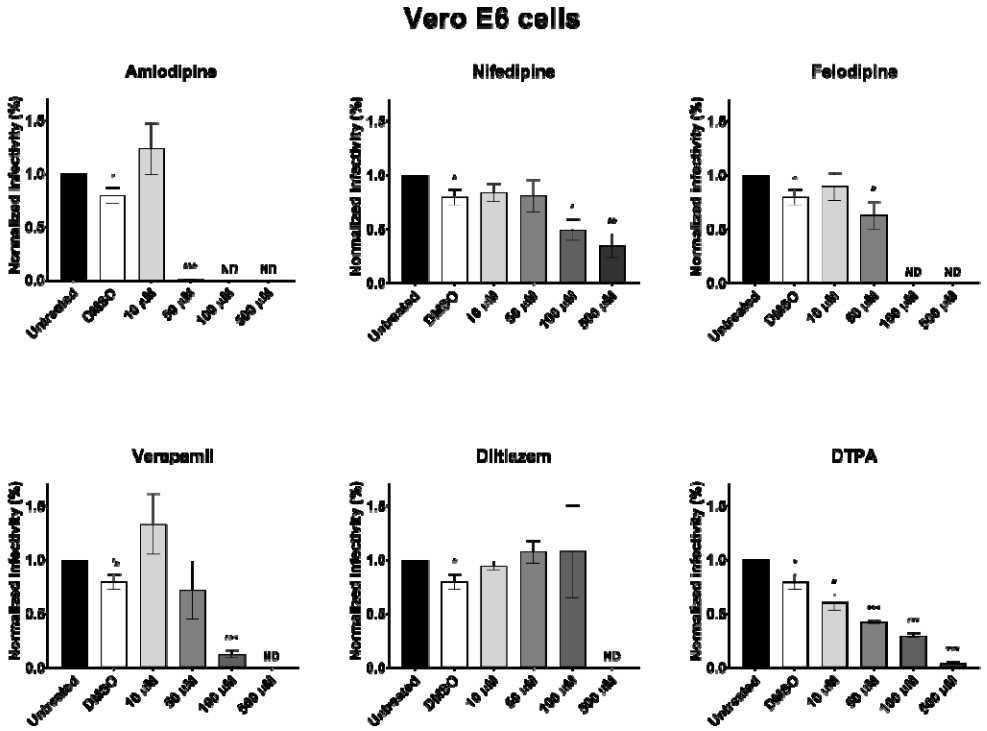

Figure 3B

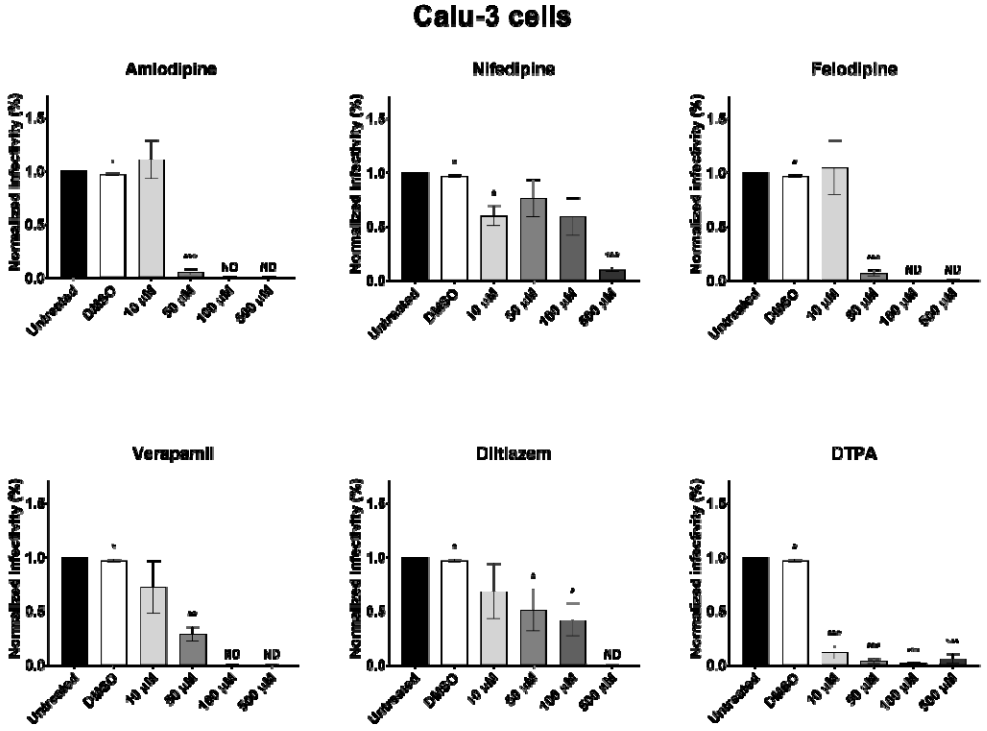

bioRxiv preprint doi: https://doi.org/10.1101/2020.07.21.214577; this version posted October 21, 2020. The copyright holder for this preprint (which was not certified by peer review) is the author/funder, who has granted bioRxiv a license to display the preprint in perpetuity. It is made available under aCC-BY-NC-ND 4.0 International license.
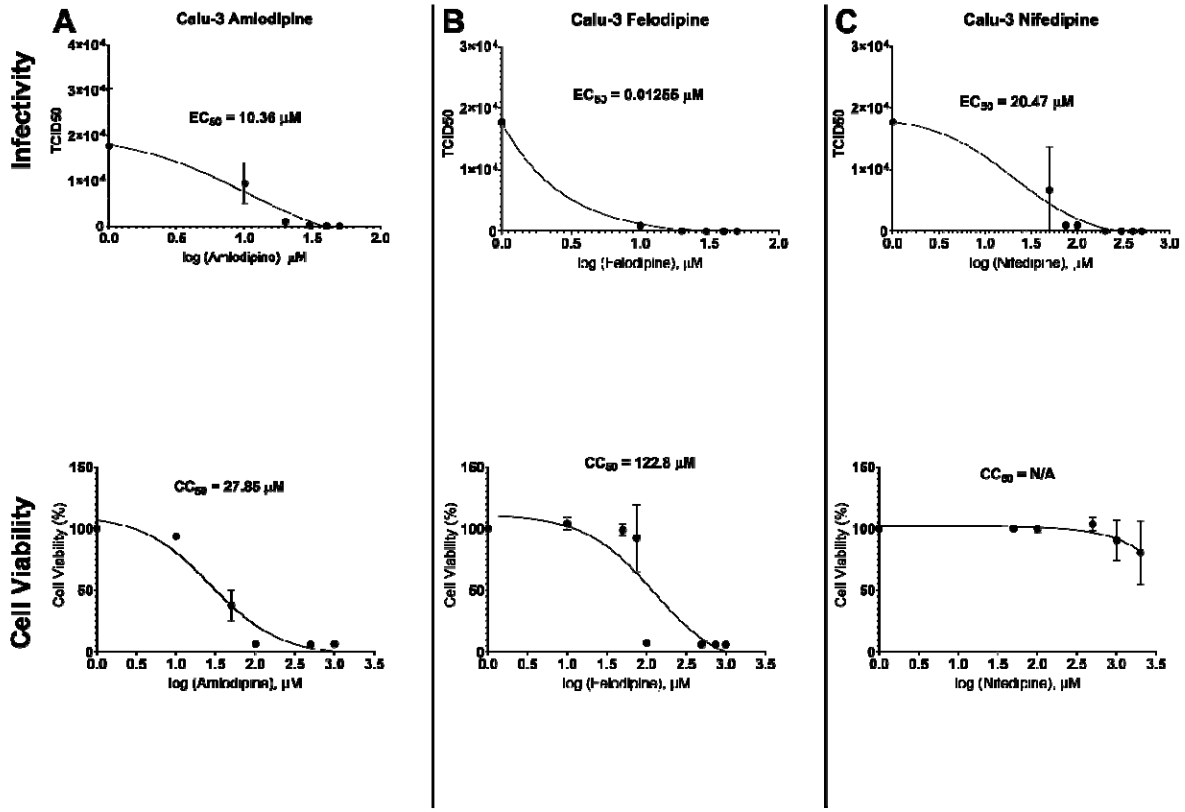
Supplemental Information Figure 1